Materials and methods

Materials

Plasmids encoding wildtype *E. coli* EF-G and its mutants (Cys-free and 196C) were constructed previously (Wilson & Noller, 1998). For the present study, EF-G mutant 58C was introduced into the Cys-free plasmid. EF-G proteins, *E. coli* 70S ribosomes, and phage T4 gene 32 mRNA were prepared as described (Wilson & Nechifor, 2004), and *N*-acetyl-Phe-tRNA (>90% purity) as described (Walker & Fredrick, 2008). Vio was provided by Julian Davies (University of British Columbia). Other reagents were purchased (from the following companies): fus, tRNAs, trypsin, and unlabeled GTP, GDP, and GDPNP (Sigma-Aldrich); [γ^{32}-P]GTP (Perkin-Elmer); mant-GDPNP, mant-GDP, and OG maleimide (Invitrogen).

Aqueous buffers contained the following components. *Buffer A:* 80 mM HEPES-KOH pH 7.7, 50 mM NH_4Cl, 10 mM $MgCl_2$, 1 mM DTT. *Buffer 1:* 10 mM Tris-HCl (pH 8.0), 100 mM KCl, 50% glycerol, 1 mM dithiothreitol (DTT). *Buffer 2:* 10 mM HEPES-KOH (pH 7.0), 100mM KCl. *Buffer 3:* 80 mM HEPES-KOH (pH 7.7), 100 mM KCl.

GTP hydrolysis and ribosome translocation

Assays were conducted in buffer A as described (Wilson & Nechifor, 2004; Nechifor *et al*, 2007; Nechifor & Wilson, 2007), with the following modifications. Vio was bound to the vacant ribosome or pretranslocation ribosome complex (20^{o}C, 15 m) before adding EF-G, while fus and GDPNP were added with EF-G. Specific reactions are described in Figure 1.

Probe attachment to EF-G

Chemical probes, OG and FeBABE, were covalently attached to the thiol group of single Cys mutants of *E. coli* EF-G (58C, 196C, and 426C), as follows.

EF-G proteins (100 μM) were transferred from buffer 1 to buffer 2 by centrifugal filtration (Millipore microcon ultracel YM-30). OG (500 μM) and limiting β-mercaptoethanol (β-ME; 25 μM) were added. Reactions were incubated in the dark (20^{o}C, overnight), and quenched with excess β-ME (100 mM). EF-G(OG) were purified

by ultrafiltration and analyzed by SDS-PAGE. Properly-folded EF-G(OG) was further purified by gel filtration chromatography (Superdex200; 10/300GL FPLC) in buffer 2, dialyzed against buffer 1, and stored at -80°C. The ratio *R* of OG attached to EF-G varied between 0.6 and 0.8, as determined by the protein's absorbance of light at 280 and 496 nm, and the equation: $R = (A_{496} \times \varepsilon_{EF\text{-}G})/(A_{280} \times \varepsilon_{OG})$, where ε_{OG} = 81,000 $M^{-1}cm^{-1}$ and $\varepsilon_{EF\text{-}G}$ = 64,282 $M^{-1}cm^{-1}$.

FeBABE was freshly prepared by mixing BABE (10 mM) and $FeSO_4$ (9 mM) in 10 μl of aqueous sodium acetate (100 mM; pH 6.0), incubated (20°C, 1 h), and quenched with EDTA (10mM). FeBABE (100 μM) and EF-G (30 μM) were mixed in buffer 3, and incubated (37°C, 15 m). EF-G(FeBABE) was purified by centrifugal filtration, and used immediately in experiments. Protein concentrations were estimated by the Bradford assay.

Structural modeling and data analysis

PyMol software (http://pymol.sourceforge.net/) was used for structural analysis and generation of molecular graphics. SigmaPlot, ImageQuant, and Microsoft Excel programs were used for data analysis.

Supplementary Table

Supplementary Table S1 N-terminal amino acid sequence of the 72-kDa fragment of EF-G (Figure 2). Sequence was determined by Edman degradation techniques.[1]

Residue	*Amino acid*	*Retention time (m)*	*Yield (pmol)*
1	Gly	6.1	49
2	Ile	18.8	7
3	Thr	5.9	5
4	Ile	18.8	4
5	Thr	5.9	2
6	Ser	5.3	1

[1] Performed at the Genome British Columbia Proteomics Centre (University of Victoria)

Supplementary Figure Legends

Supplementary Figure S1 Comparison of the sw1 elements of EF-G and EF-Tu. The amino acid sequence of sw1 of *E. coli* EF-G is aligned to the homologous sequences of EF-G, EF-G-2, and EF-Tu from *T. thermophilus* and *T. aquaticus*, whose crystal structures in the GDPNP(free) and GDP(free) states have been determined (Supplementary Figure S6). Residue numbers (above) refer to *E. coli* EF-G.

Supplementary Figure S2 Trypsin cannot access sw1 of ribosome-bound EF-G in the GDPNP state. (**A**) Trypsin docked onto ribosome-bound EF-G. The electron density map (contoured at 3σ), and the underlying structural model, is based on a cryo-EM structure of *T. thermophilus* EF-G-2•GDPNP•ribosome (Connell *et al*, 2007). EF-G-2 is shown in yellow, trypsin in blue, its active-site Ser residue in red, sw1 of EF-G-2 in tan, and the ribosome in white. (**B**) Orthogonal view of panel (A), with the ribosome invisible. The Ser residue (*red*) in the active site of trypsin cannot access the scissile peptide bond (*red*) of EF-G.

Supplementary Figure S3 Functional activities of EF-G proteins conjugated with FeBABE. (**A**) GTP hydrolysis. Reactions were conducted with proteins 58C-FeBABE and 196C-FeBABE, under single-turnover conditions, as described in Figure 1(B). Products were analyzed by thin layer chromatography. (**B**) Ribosome translocation. Reactions were conducted as described in Figure 1. Products were analyzed by toeprinting (Wilson & Nechifor, 2004).

Supplementary Figure S4 Directed hydroxyl radical probing of sw1 movement in the ribosome. Reactions were conducted as described in Figure 4(A). Products were analyzed by primer extension. Shown here are results of cleavages identified in elements of 16S rRNA. Solid and broken rectangles (*right*) identify strongly and weakly cleaved rRNA nucleotides, respectively. Other labels are identified in the legend to Figure 4A. The strongly cleaved 16S rRNA nucleotides, as identified in these gels, map to helices 5, 8, and 14. These nucleotides are on the face of the 30S subunit, directly across from helix 95 of 23S rRNA, as shown in Figure 4B.

Supplementary Figure S5 Kinetics of release of nucleotide and EF-G from the ribosome. (**A**) Release of fluorescent nucleotide from ribosome-bound EF-G. Wildtype E. coli EF-G was bound to the vacant ribosome in the presence of mant-GTP and either fus (100 μM) or vio (100 μM). Experiments were otherwise conducted as described in Figure 5A. (**B**) Release of fluorescent EF-G from the ribosome. EF-G(426C), conjugated with OG fluorophore, was bound to the vacant ribosome in the presence of mant-GTP and either fus (100 μM) or vio (100 μM). Experiments were otherwise conducted as described in Figure 5(B). In panels A and B, results obtained using the GDP/vio complex are shown in red. Those using the GDP/fus complex are shown in blue.

Supplementary Figure S6 Sw1 conformational changes in EF-G, and EF-Tu. *Red:* sw1 element, and conserved Thr and Gly residues of sw1 and sw2, respectively. *Yellow:* G domains. Structures are based on the following PDB IDs (http://www.rcsb.org/pdb/home/home.do): 1WDT, 2BM1, 1EFT, and 1TUI. Note that residues 57–65 of sw1 of EF-G(G16V) •GDP were unintentionally left out of the original file 1BKD. These residues are included here, based on the crystallographic data (Hansson *et al*, 2005; and D Logan, personal communication).

References

Connell SR , Takemoto C , Wilson DN , Wang H , Murayama K , Terada T, Shirouzu M , Rost M , Schuler M , Giesebrecht J , Dabrowski M , Mielke T , Fucini P , Yokoyama S , Spahn CM (2007). Structural basis for interaction of the ribosome with the switch regions of GTP-bound elongation factors. *Mol Cell* **25**(5): 751-764

Hansson S , Singh R , Gudkov AT , Liljas A , Logan DT (2005) Structural insights into fusidic acid resistance and sensitivity in EF-G. *J Mol Biol* **348**(4) 939-949

Nechifor R, Murataliev M, Wilson KS (2007) Functional interactions between the G' subdomain of bacterial translation factor EF-G and ribosomal protein L7/L12. *J Biol Chem* **282**: 36998-37005

Nechifor R, Wilson KS (2007) Crosslinking of translation factor EF-G to proteins of the bacterial ribosome before and after translocation. *J Mol Biol* **368**: 1412-1425

Walker SE, Fredrick K (2008) Preparation and evaluation of acylated tRNAs. *Methods* **44**: 81-86

Wilson KS, Nechifor R (2004) Interactions of translational factor EF-G with the bacterial ribosome before and after mRNA translocation. *J Mol Biol* **337**: 15-30

Wilson KS, Noller HF (1998) Mapping the position of translational elongation factor EF-G in the ribosome by directed hydroxyl radical probing. *Cell* **92**: 131-139

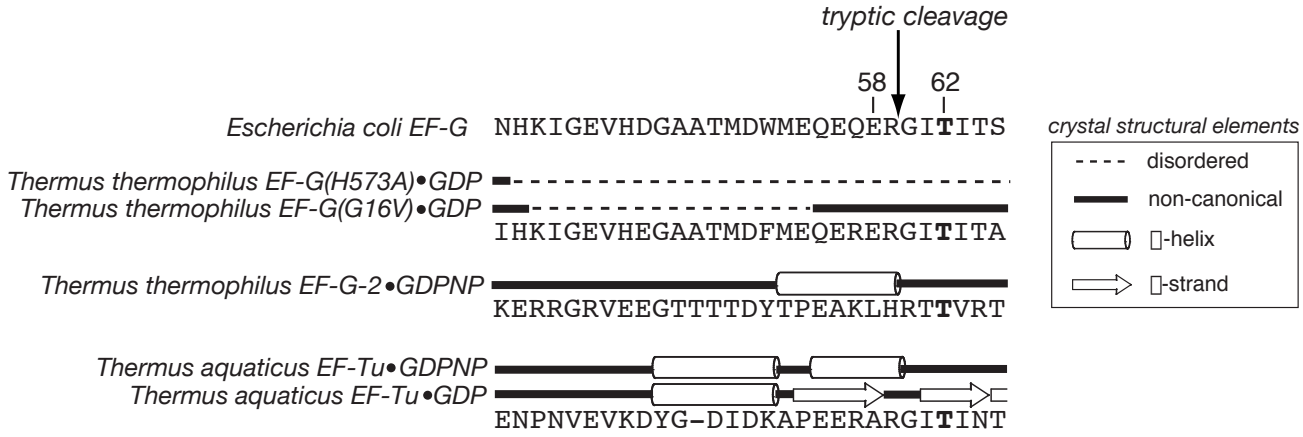
tryptic cleavage
58
62
Escherichia coli EF-G NHKIGEVHDGAATMDWMEQEQERGITITS
Thermus thermophilus EF-G(H573A)•GDP
Thermus thermophilus EF-G(G16V)•GDP
IHKIGEVHEGAATMDFMEQERERGITITA
Thermus thermophilus EF-G-2•GDPNP
KERRGRVEEGTTTTDYTPEAKLHRTTVRT
Thermus aquaticus EF-Tu•GDPNP
Thermus aquaticus EF-Tu•GDP
ENPNVEVKDYG-DIDKAPEERARGITINT
crystal structural elements
disordered
non-canonical
-helix
-strand

Supplementary Figure S2

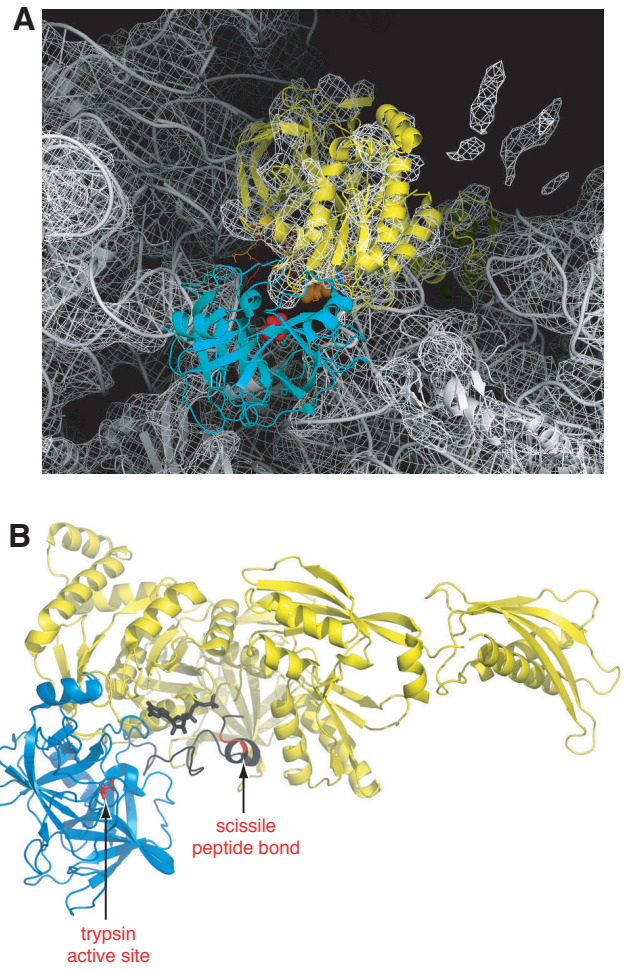

Supplementary Figure S3

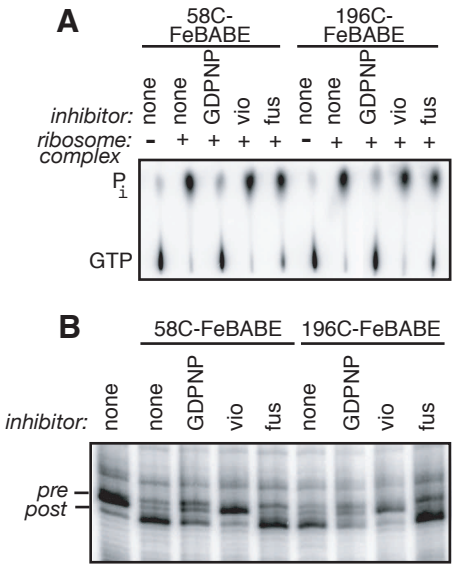

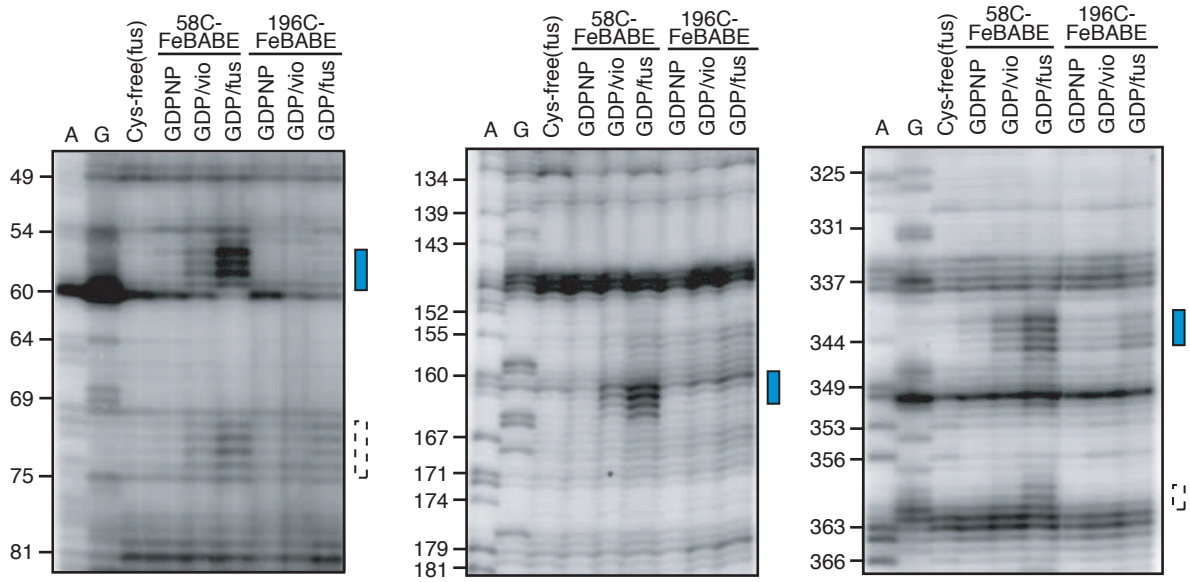
A
G
Cys-free(fus)
58C-FeBABE
196C-FeBABE
GDPNP
GDP/vio
GDP/fus
49
54
60
64
69
75
81
134
139
143
152
155
160
167
171
174
179
181
325
331
337
344
349
353
356
363
366

Supplementary Figure S5

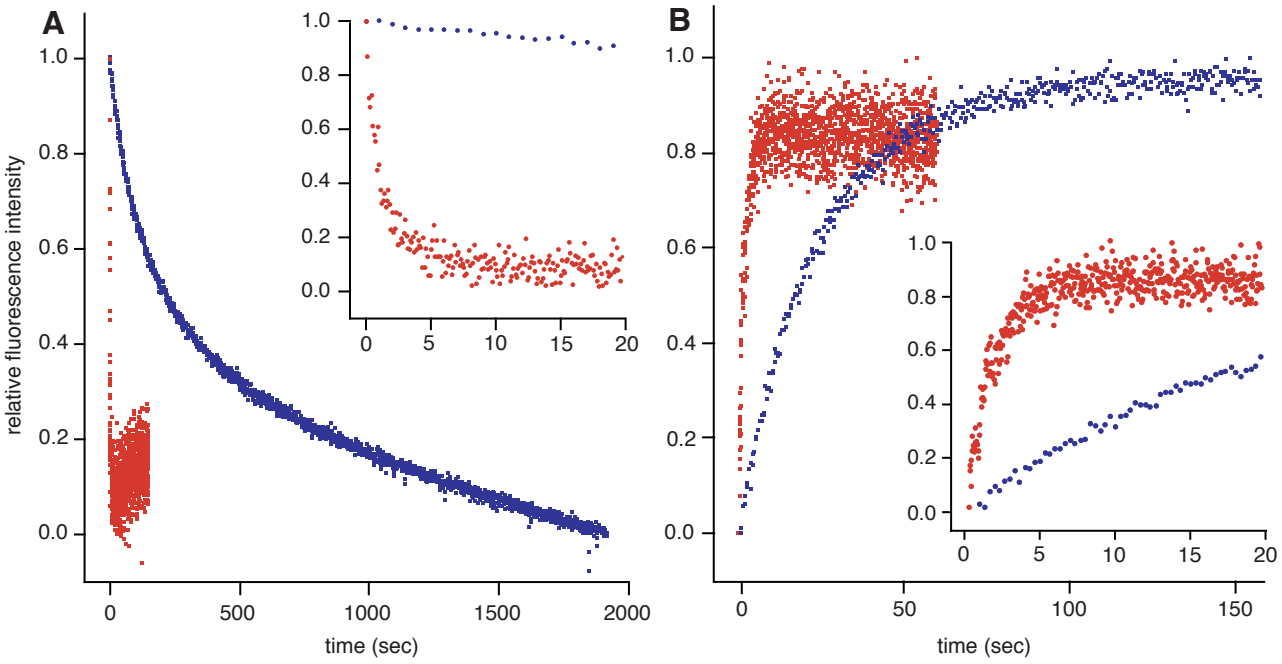

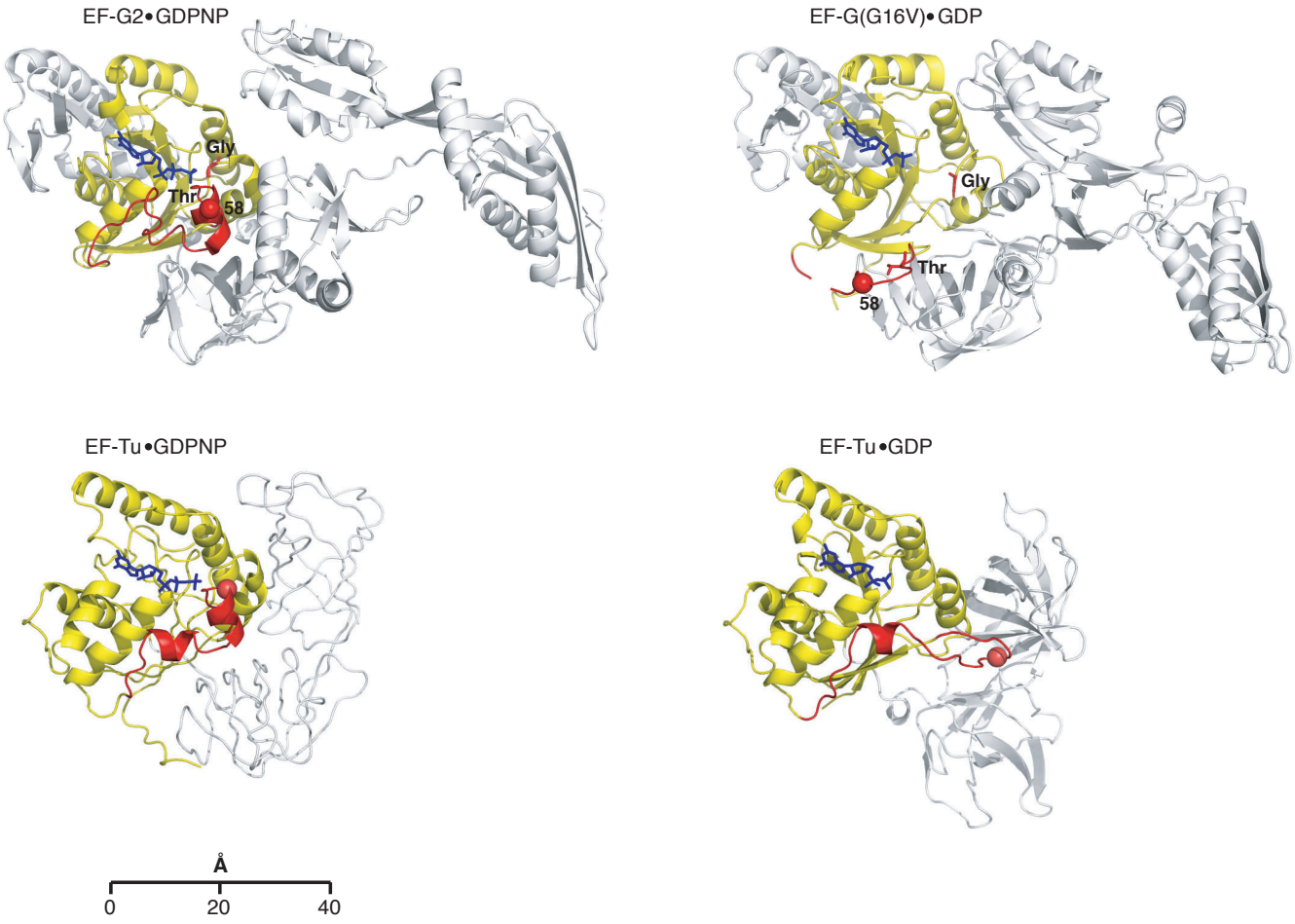
EF-G2•GDPNP
Gly
Thr
58
EF-G(G16V)•GDP
Gly
Thr
58
EF-Tu•GDPNP
EF-Tu•GDP
Å
0
20
40